Rare Metal Materials and Engineering
Volume 50, Issue 10, October 2021
Available online at www.rmme.ac.cn

Science Press

Cite this article as: Sun Zhiyong, Liu Fenjun, Chen Haiyan. Influence of Friction Stir Processing with the Same Speed Ratio on Microstructure Evolution, Mechanical Properties and Corrosion Performances of Stirred Zone in Al-Mg-Si Alloy[J]. Rare Metal Materials and Engineering, 2021, 50(10): 3454-3461.

ARTICLE

Influence of Friction Stir Processing with the Same Speed Ratio on Microstructure Evolution, Mechanical Properties and Corrosion Performances of Stirred Zone in Al-Mg-Si Alloy

Sun Zhiyong[1], Liu Fenjun[1,2], Chen Haiyan[3]

[1] College of Energy Engineering, Yulin University, Yulin 719000, China; [2] Yulin Key Laboratory of Metal Matrix Composites and Remanufacturing Technology, Yulin University, Yulin 719000, China; [3] School of Materials Science and Engineering, Northwestern Polytechnical University, Xi'an 710072, China

Abstract: Friction stir processing (FSP) was applied to process a 2 mm thick Al-Mg-Si (6061-T6) alloy plate. The influence of the FSP with the same speed ratio on microstructure evolution, microhardness distribution, tensile properties and corrosion performances of the stirred zone (SZ) in the 6061-T6 alloy was investigated. Results show that there are obvious differences in the microstructure, such as grain morphologies, mean grain size, grain boundary distributions and precipitate distributions of the SZ prepared using the FSP with different processing speeds, which in turn affects the mechanical properties and corrosion resistance. The mean grain size of the equiaxed recrystallized grains of the SZ sample prepared by high speed (8000 r/min, 800 mm/min) is 9.5 μm, which is significantly refined compared to 23.2 μm of the conventional speed (1000 r/min, 100 mm/min) and 13.6 μm of the as-received 6061-T6 alloy. In addition, the distribution characteristics of the precipitates are more similar to that of the as-received 6061-T6 alloy. As a result, in addition to the slight change in corrosion resistance, the SZ sample prepared using the high speed FSP exhibits excellent mechanical properties. The maximum tensile strength and elongation of the SZ sample are 281.5 MPa and 34.8%, which are 86.3% and 122.1% of that of the as-received 6061-T6 alloy, respectively.

Key words: Al-Mg-Si alloy; friction stir processing; microstructure evolution; mechanical properties; corrosion performance

Al-Mg-Si (6061-T6) alloys have been widely applied in structural components, such as aerospace, train and shipbuilding, for reducing mass due to their low densities and relatively high strength[1,2]. As a precipitation-strengthened aluminum alloy, the mechanical properties and corrosion resistance of the 6061-T6 alloy mainly depend on the distribution characteristics of precipitates, followed by the mean grain size[3]. The precipitate distribution and grain refinement can enhance the tensile properties of the 6061-T6 alloy based on the well-known solid solution strengthening and Hall-Petch relation[4,5]. Although aluminum alloys have good corrosion resistance, the precipitates, such as Mg_2Si in the 6061-T6 alloy, distributed at the grain boundaries may induce the susceptibility to intergranular corrosion[6]. It is urgent to develop a processing technology that can not only refine the grain size, but also improve the distribution characteristics of precipitates.

Friction stir processing (FSP), as a solid-state processing technology, can change the grain size and precipitate distributions by adjusting the processing conditions[7,8], such as processing parameters[9], tool geometries[10,11], cooling condition[12,13], and adding nano-sized ceramics[14] and alloy particles[15] in the processed area. Mohamadigangaraj et al[16] assessed the effect of rotating speed and number of FSP passes on the mechanical properties of aluminum alloy using the response surface methodology and found that the

Received date: June 01, 2021
Foundation item: National Natural Science Foundation of China (51861034, 52064048); Science and Technology Department of Shaanxi Province (2020GY-262); Science and Technology Bureau of Yulin (2019-86-1, CXY-2020-006-01); High-Level Talent Project of Yulin University (20GK06)
Corresponding author: Chen Haiyan, Ph. D., Associate Professor, School of Materials Science and Engineering, Northwestern Polytechnical University, Xi'an 710072, P. R. China, E-mail: hychen@nwpu.edu.cn

microhardness and mechanical properties increase with increasing the rotating speed and the number of FSP passes. Woo et al[17] investigated the influence of the tool geometries on microstructural softening during FSP and found that the microstructural softening is mainly attributed to the frictional heat input between the workpiece and tool shoulder, which causes the dissolution and growth of the precipitates and further reduces the microhardness. Chen et al[18] ascertained the effect of water cooling on the microstructure and mechanical properties of FSP 6061 alloy and found that its influence mainly depends on the initial tempering of 6061 alloy. The stirred zone (SZ) prepared by FSP with water cooling is significantly strengthened for natural-aged 6061 alloy due to grain refinement, high density of dislocations and a large number of fine precipitates, whereas it is less strengthened for the annealed 6061 alloy due to little microstructure difference. Zhao et al[19] investigated the effect of FSP with B4C particles on the grain size, particle distributions and microhardness of the SZ in the 6061 alloy and found that the average microhardness value increases due to grain refinement and uniform particle distributions. In addition to microstructure evolution and mechanical properties, some researchers also paid attention to the corrosion properties of the FSP aluminum alloy. Barati et al[20] adopted FSP and FSP with vibration to adjust the surface microstructure of the 6061 alloy by adding or not adding SiO_2 strengthening nanoparticles. The SZ prepared by FSP with vibration by adding SiO_2 strengthening nanoparticles is better than that prepared by FSP due to the finer grain size and more uniform distribution of SiO_2 strengthening nanoparticles. They also investigated the influence of passes number on the microstructure evolution and corrosion resistance of the SZ with SiO_2 strengthening nanoparticles in the 6061 alloy, and found that the SZ presents more homogenous distribution of the SiO_2 strengthening nanoparticles and coarsening of Mg_2Si precipitates by increasing the passes number[21]. As a result, the SZ exhibits worse corrosion properties due to coarsening of Mg_2Si precipitates and grain refinement[21]. Although FSP can improve the mechanical properties and corrosion resistance of aluminum alloy by adjusting the microstructure of the SZ, most of the published research reports are based on conventional rotating speed and travelling speed. That is, the rotating speed and travelling speed are typically less than 2000 r/min and 200 mm/min, respectively. However, there are few reports on the microstructure evolution, mechanical properties and corrosion behavior of the SZ in aluminum alloy prepared by high rotating speed FSP.

The present work aimed to prepare the sound SZ in 6061-T6 alloy with excellent mechanical properties and corrosion performances by high rotating speed FSP technology. At the same time, the microstructure evolution of the SZ in the FSP process was studied to elucidate the mechanical properties and corrosion behavior.

1 Experiment

1.1 Materials and FSP procedure

The as-received material used in the present work was 2 mm thick commercial 6061-T6 alloy with a chemical composition (wt%) of 0.40~0.80 Si, 0.7 Fe, 0.15~0.40 Cu, 0.15 Mn, 0.80~1.20 Mg, 0.04~0.35 Cr, 0.25 Zn, 0.15 Ti, and Al balance. The FSP samples with dimensions of 180 mm in length and 100 mm in width were prepared using a wire electro-discharge machining (WEDM). The FSP operation was conducted using a dedicated high-speed FSW-TS-F08-DZ FSW machine. A tool used in the present FSP was made of H13 tool steel, which comprised a 10 mm diameter shoulder with a three helical concave surface of 5° and a 1.5 mm long cone-shaped pin. The top and root diameters of the pin were 3 and 2 mm, respectively. A single pass FSP with the same speed ratio was performed along the rolling direction with a tool inclination angle of 0° , and the processing parameters applied in this study are listed in Table 1. The samples were named based on the processing condition; for instance, the sample fabricated using a rotating speed of 1000 r/min and travelling speed of 100 mm/min was labeled as 1000-100.

1.2 Microanalysis

After FSP operation, the SZ was sectioned perpendicular to the processing direction and then prepared by standard metallographic techniques. Then, the sample obtained from the central portion of the SZ was used for microstructure examination, corrosion and hardness tests. Texture development was examined using an electron backscatter diffraction (EBSD, HKL Channel 5 System). The precipitate evolution in the SZ was observed using a transmission electron microscope (TEM, FEI TECANI-F30) operated at 200 kV after electropolishing. The electrochemical testing was performed using a VERSASTAT 400 three-electrode electrochemical workstation, which was conducted on the SZ surface with a 1 cm^2 testing area. The working, reference and auxiliary electrodes were the SZ, a saturated Ag/AgCl electrode and platinum, respectively. The hardness distribution was measured using a HMV-1 hardness tester, along mid-thickness of the SZ using a load of 0.98 N and a dwell time of 10 s with a distance of 0.25 mm between indents. It should be noted that the hardness measurement was conducted after sufficient natural aging (4 weeks). The tensile testing was conducted on an INSTRON 3382 universal testing machine, using a standard specimen with a width of 6 mm obtained from the SZ parallel to the tool travel direction, and a constant cross head speed of 1.0 mm/min.

2 Results and Discussion

2.1 Surface morphology and microstructure

Fig. 1 shows the surface morphologies of the SZ on 6061-

Table 1 FSP parameters applied in the present study

Sample	Rotating speed/r·min^{-1}	Travelling speed/mm·min^{-1}
1000-100	1000	100
2000-200	2000	200
4000-400	4000	400
8000-800	8000	800

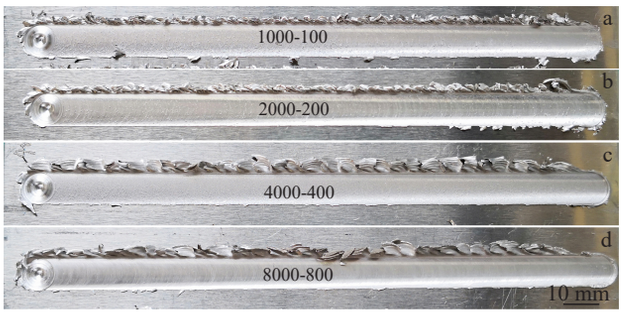

Fig.1 Surface morphologies of the SZ on 1000-100 (a), 2000-200 (b), 4000-400 (c) and 8000-800 (d) samples

T6 alloy prepared using FSP with the same speed ratio. In addition to the defect-free, it can be also seen that the sound SZ on 6061-T6 alloy becomes smooth and flat with increasing the rotating speed and travelling speed. It means that the selected rotating speed and travelling speed used in this study are reasonable, which can produce a sufficient heat input to enhance a balanced material flow[22]. As a result, the SZ with defect-free is produced in the processed zone.

The microstructure characteristics, including grain morphologies, grain size distributions, grain boundary distributions, grain type distributions and precipitate evolution, of the 6061-T6 alloy and SZ prepared by FSP with the same speed ratio are presented in Fig. 2~5. It can be seen that the grains in the as-received 6061-T6 alloy are elongated along the rolling direction and presents a pancake-shaped grain morphology, as shown in Fig. 2a. The mean grain size and high angle grain boundaries (HAGBs) of the as-received 6061-T6 alloy are 13.6 μm and 92.2% according to the grain size distributions and grain boundary distributions, as shown in Fig. 2b and 2c, respectively. The grain type distributions indicate that the as-received 6061-T6 alloy is mainly composed of recrystallized grains, which is about 96.0%, as shown in Fig. 3a. After FSP, the SZ of the 6061-T6 alloy is characterized by equiaxed grains, as shown in Fig. 2d, 2g and 2j. With the increase of the rotating speed and travelling speed, the mean grain size of the SZ gradually decreases (Fig. 2e, 2h and 2k), whereas the proportions of the HAGBs and recrystallized grains gradually increase, as shown in Fig. 2f, 2i, 2l, respectively. The mean grain sizes of the SZ on the 1000-100, 4000-400 and 8000-800 samples are 23.2, 10.5 and 9.5 μm, respectively. And the SZ of the 1000-100 sample prepared by conventional processing speed consists of 31.4% recrystallized grains, but the SZ of the 4000-400 and 8000-800 samples prepared by high processing speed consists of 42.7% and 65.1% recrystallized grains, respectively, as shown in Fig. 4. The number and size of the Mg_2Si, Al_8Fe_2Si and Al_2CuMg precipitates significantly increase with the increase of the rotating speed and travelling speed with the same speed ratio, as shown in Fig. 5. The precipitates in the as-received 6061-T6 alloy are Mg_2Si, Al_8Fe_2Si and Al_2CuMg, as shown in Fig. 5a. The specific characteristics of the Mg_2Si, Al_8Fe_2Si and Al_2CuMg precipitates have been determined in our previous researches[23]. Furthermore, the precipitate distributions of the Mg_2Si, Al_8Fe_2Si and Al_2CuMg, such as the number, morphology and size, are more similar to that of the as-received 6061-T6 alloy with increasing the rotating speed and travelling speed, as shown in Fig. 5b~5d. This phenomenon is consistent with what we have previously discovered in the friction stir welding of 6061-T6 alloy[24]. The number of precipitates in the nugget zone produced by high speed friction stir welding is obviously larger than by conventional speed friction stir welding, and the distribution is more dispersed and homogenized[24]. It can be seen that in addition to the most similar distributions of the precipitates with the 6061-T6 alloy, the SZ of the 8000-800 sample exhibits the finest mean grain size and the largest proportions of the HAGBs and recrystallized grains, which are 9.5 μm, 58.7% and 65.1%, respectively.

It is well known that the microstructure evolution of the SZ during FSP mainly depends on the processing heat input, which is mainly caused by the rotating speed and travelling speed. The peak temperature (T) of the SZ can be evaluated by the rotating speed (ω), travelling speed (v) and the melting temperature (T_m) of the 6061-T6 alloy[25].

$$T = K\left(\frac{\omega^2}{v\cdot 10^4}\right)^{\alpha}\cdot T_m \quad (1)$$

where K and α are constants.

Based on Eq.(1), the influence of rotating speed on the peak temperature of the SZ is greater than that of the travelling speed. As a result, even if the same speed ratio is used in the process of the FSP, the peak temperature will increase with increasing the rotating speed. In this way, the dissolution and reprecipitation of the precipitates in the SZ during the heating and cooling stages are more sufficient in the high rotating speed FSP, making the precipitate distributions more similar to that of the as-received 6061-T6 alloy. In general, the higher the temperature of the SZ, the larger the mean grain size. However, in the present work, it is found that the mean grain size gradually decreases with the increase of the rotating speed. In fact, the mean grain size of the SZ not only depends on the heat input, but also on the strain rate. Previous studies have demonstrated that the mean grain size of the SZ decreases as increasing the strain rate[25,26]. In the present work, the SZ prepared using high rotating speed FSP is characterized by finer mean grain size, which indicates that the strain rate is the main factor influencing the grain refinement of the high rotating speed FSP. In addition, the higher heat input and greater strain rate can cause more complete recrystallization in the SZ, resulting in a significant increase in the proportions of the HAGBs and recrystallized grains. An interesting phenomenon in the present study is that the heat input of the 1000-100 sample is smaller than that of the 8000-800 sample according to Eq.(1), but the mean grain size of the 1000-100 sample is significantly larger than that of the 8000-800 sample. This means that the mean grain size of the SZ prepared by conventional rotating speed FSP mainly depends on the heat input rather than on the strain rate. Generally, this

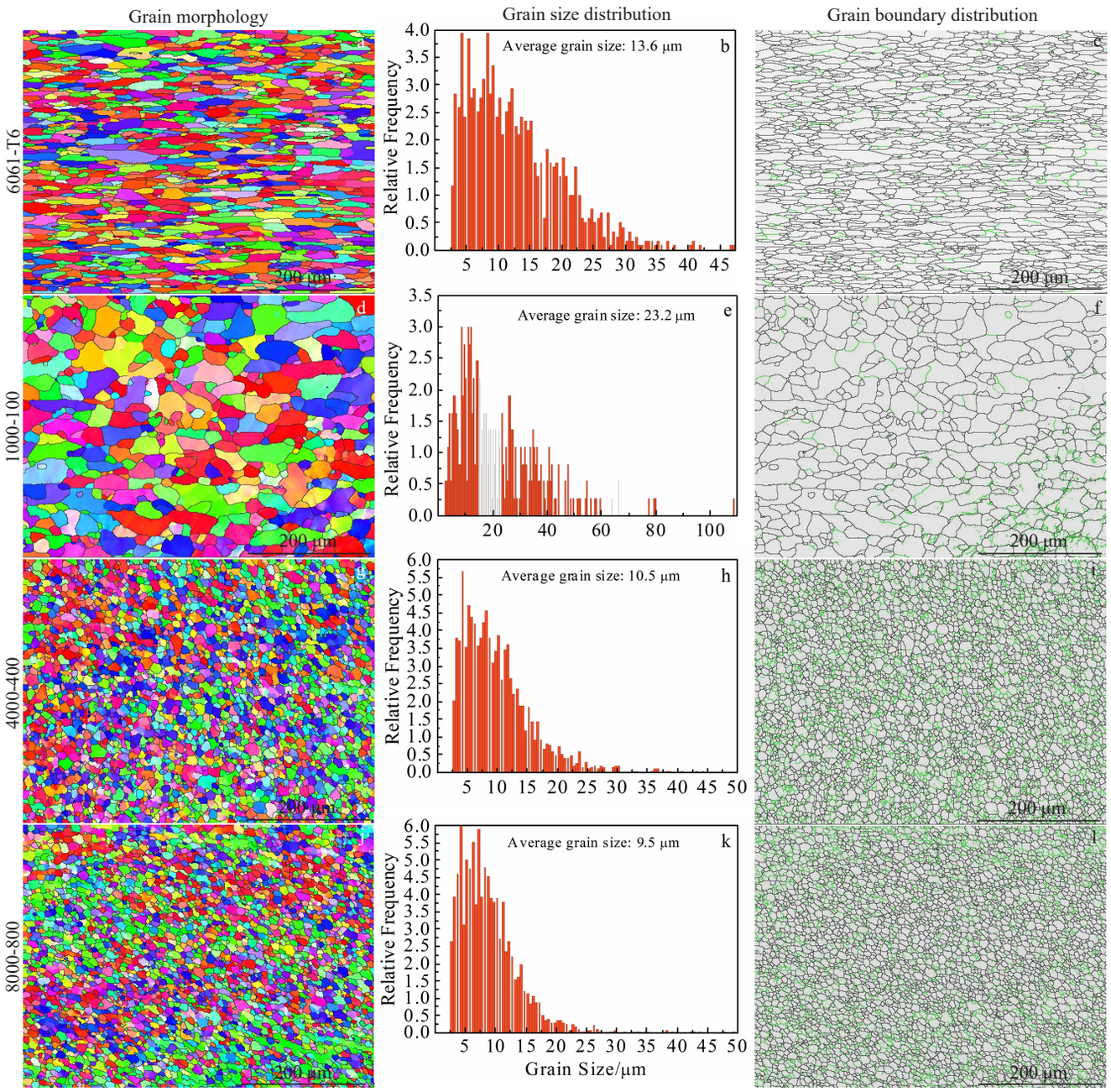

Fig.2 Microstructure characteristics of 6061-T6 alloy (a, b, c) and samples of 1000-100 (d, e, f), 4000-400 (g, h, i) and 8000-800 (j, k, l)

phenomenon of microstructural instability at high temperatures is commonly found in post heat-treated friction stir welded aluminum alloys, such as 6061[27] and 6082[28,29]. This abnormal grain growth phenomenon is often explained in terms of Humphreys's cellular model[30,31]. Jandaghi et al[32] investigated the influence of the solution treatment on the interfacial phase evolutions of the dissimilar friction stir welded joints of AA2198-AA7475 and AA2198-AA6013, and found that the ultrafine grains of the SZ are the initiation sites for abnormal grain growth. The ultrafine grains of the SZ experience the most serious abnormal growth during treatment at elevated temperatures. As a result, the ultrafine grains in the SZ are significantly coarser after solution treatment[32].

2.2 Mechanical properties

The microhardness distributions and tensile strength significantly smaller of the 6061-T6 and SZ samples prepared by FSP with the same speed ratio are shown in Fig. 6. The mean microhardness value of the SZ is significantly smaller than that of the as-received 6061-T6 alloy, as shown in Fig.6a. The mean microhardness value of the SZ produced using high rotating speed FSP is obviously greater than that of the SZ prepared using conventional rotating speed FSP. However, the microhardness distribution of the SZ prepared using high rotating speed FSP exhibits little difference. The average

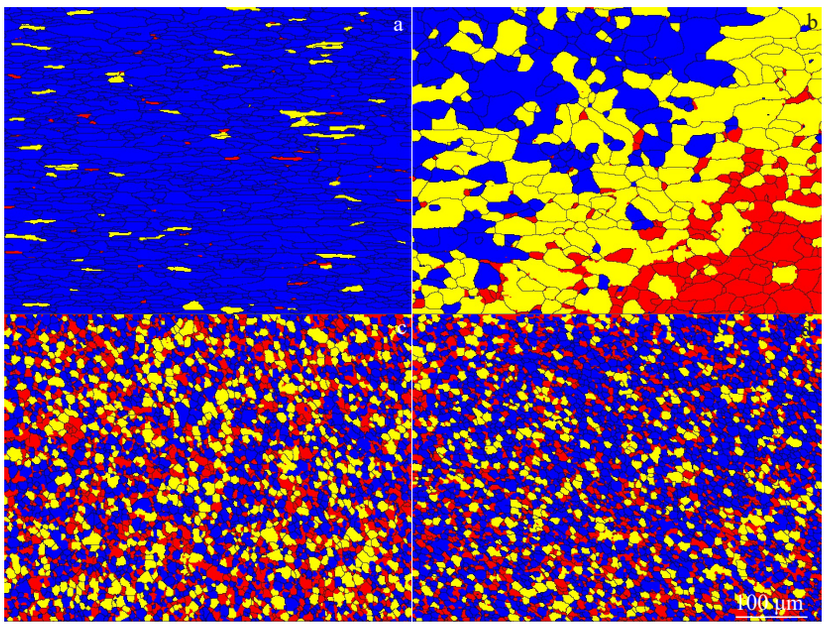

Fig.3 Grain type distributions of the 6061-T6 alloy (a) and samples of 1000-100 (b), 4000-400 (c) and 8000-800 (d)

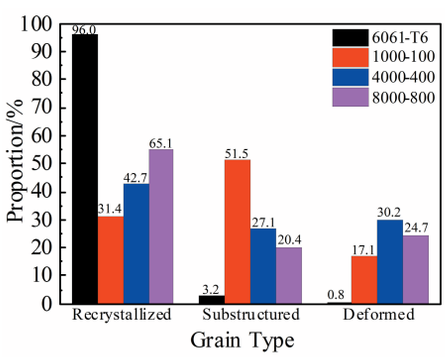

Fig.4 Grain type proportion of 6061-T6 and the SZ samples obtained corresponding to Fig.3

microhardness value of the SZ of the 1000-100 sample is 610 MPa, but the mean microhardness value of the SZ of the 4000-400 and 8000-800 samples are 860 and 868 MPa, respectively. The tensile test results indicate that the tensile strength of the SZ sample is smaller than that of the 6061-T6 alloy, whereas the elongation of the SZ produced by high rotating speed FSP is greater than that of the 6061-T6 alloy, as shown in Fig. 6b. The SZ of the 8000-800 sample exhibits excellent tensile properties. The maximum tensile strength of 281.5 MPa and elongation of 34.8% are obtained in the SZ of the 8000-800 sample, which are 86.3% (326.0 MPa) and 122.1% (28.5%) of the 6061-T6 alloy, respectively. The minimum tensile strength of 195.1 MPa and elongation of 22.7% are obtained in the SZ of the 1000-100 sample, which are 59.8% and 79.6% of the 6061-T6 alloy, respectively. According to the tensile properties of the SZ, it can be inferred that high rotating speed FSP is more conducive to enhancing the mechanical properties of the 6061-T6 alloy compared to conventional rotating speed FSP.

According to the existing research results, the microhardness and tensile strength of the 6061-T6 alloy, as a precipitation-strengthened aluminum alloy, mainly depend on the distribution characteristics of precipitates, while its elongation mainly depends on the mean grain size[3-5]. The precipitates in the SZ are smaller than that of the 6061-T6 alloy, resulting in obviously lower average microhardness value and tensile strength of the SZ. However, the precipitate distributions in the SZ prepared by high rotating speed FSP are more similar to that of the 6061-T6 alloy compared to conventional rotating speed FSP, resulting in the significant increase in the average microhardness value and tensile strength of the high rotating speed FSP SZ. In addition, the SZ produced using high rotating speed FSP has a finer mean grain size, resulting in a larger elongation of the SZ.

2.3 Corrosion resistance

Fig. 7 presents potentiodynamic polarization and Nyquist curves of the 6061-T6 alloy and SZ produced using FSP with the same speed ratio in 3.5 wt% NaCl aqueous solution. The self-corrosion potential and self-corrosion current of the 6061-T6 alloy and SZ are estimated according to the cathodic extrapolation method of Tafel curve[33], as shown in Table 2. The self-corrosion potential of the 6061-T6 alloy and SZ on 1000-100, 2000-200, 4000-400 and 8000-800 samples are -0.56, -0.54, -0.56, -0.92 and -0.96 V, and the self-corrosion current are 7.59×10^{-6}, 1.41×10^{-5}, 2.24×10^{-6}, 1.78×10^{-6} and 4.90×10^{-6} A, respectively. The maximum self-corrosion potential and minimum self-corrosion current of the SZ are -0.54 V (1000-100 sample) and 1.78×10^{-6} A (4000-400 sample), which are 96.4% and 23.5% of that of the 6061-T6 alloy, respectively. It can be seen that the SZ prepared by the conventional rotating speed FSP has good self-corrosion

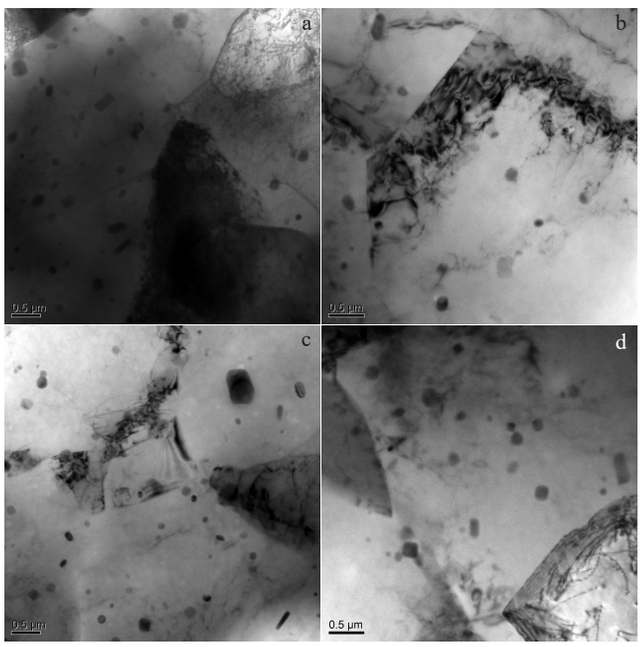

Fig.5 Precipitate distributions of 6061-T6 alloy (a) and samples of 1000-100 (b), 4000-400 (c) and 8000-800 (d)

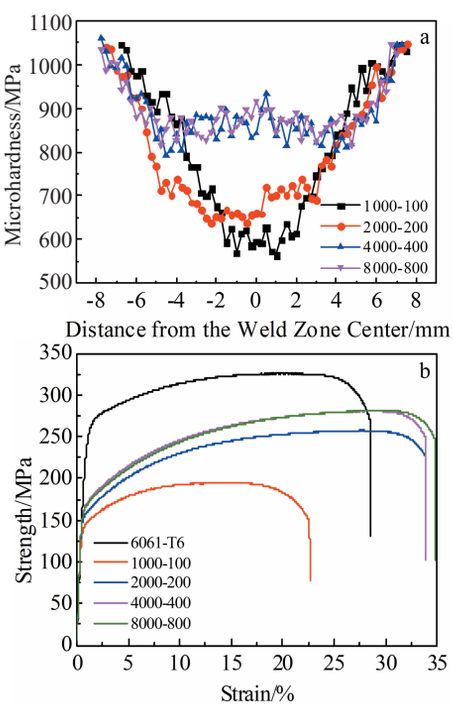

Fig.6 Microhardness distributions of SZ samples (a) and tensile strength (b) of the 6061-T6 alloy and SZ

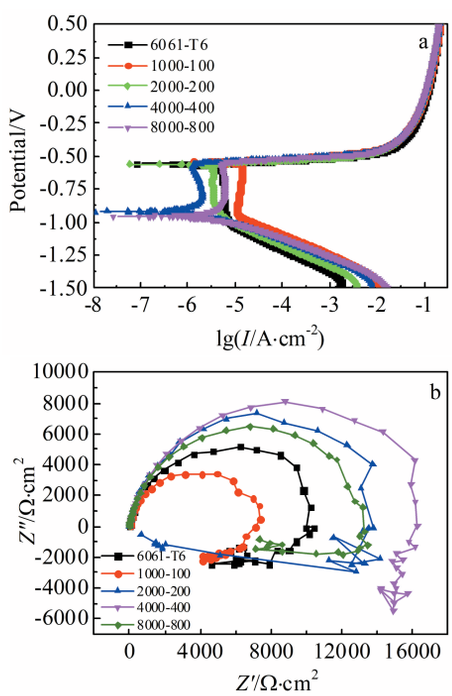

Fig.7 Potentiodynamic polarization curves (a) and Nyquist (b) curves of the 6061-T6 alloy and SZ samples

potential and poor self-corrosion current, while the SZ prepared by the high rotating speed FSP has poor self-corrosion potential and good self-corrosion current. Previous research results have demonstrated that the larger the diameter of capacitive loop, the smaller the corrosion rate[34]. The SZ prepared using high rotating speed FSP have larger diameter of capacitive loop, which means that they have smaller self-corrosion current.

The corrosion resistance of the 6061-T6 alloy is mainly affected by the precipitate distribution and grain size[35]. When the precipitates with moderate size are uniformly distributed or the average grain size is significantly refined, the 6061-T6 alloy can exhibit excellent corrosion performance. In the present work, the SZ prepared using conventional rotating

Table 2 Self-corrosion potential and self-corrosion current of the 6061-T6 and SZ sample calculated according to the cathodic Tafel extrapolation

Sample	Self-corrosion potential/V	Self-corrosion current/ $\times 10^{-6}$ A
6061-T6	-0.56	7.59
1000-100	-0.54	14.1
2000-200	-0.56	2.24
4000-400	-0.92	1.78
8000-800	-0.96	4.90

speed FSP, such as 1000-100 sample, has a larger average grain size and fewer precipitates, resulting in worse self-corrosion current. The SZ prepared using high rotating speed FSP, such as 4000-400 and 8000-800 samples, has a finer average grain size and more precipitates, resulting in better self-corrosion current.

3 Conclusions

1) FSP with the same speed ratio is successfully applied to process 6061-T6 alloy plate. The sound stirred zone (SZ) is obtained using high rotating speed FSP or conventional rotating speed FSP. The SZ sample prepared using high rotating speed FSP is smoother and flatter than using conventional rotating speed FSP.

2) Compared with conventional rotating speed FSP, the SZ in the process of high rotating speed FSP is subjected to greater heat input and stronger plastic strain, resulting in more complete recrystallization. As a result, there are finer mean grain sizes, a larger proportion of HAGBs and more precipitates with more uniform distribution in the SZ.

3) In addition to the slight change in corrosion resistance, the SZ sample prepared using high rotating speed FSP exhibits greater microhardness value, larger tensile strength and elongation compared to that of the SZ sample prepared using conventional rotating speed FSP.

References

1 Dursun T, Soutis C. *Materials Design*[J], 2014, 56(4): 862

2 Zhang X, Chen Y, Hu J. *Progress in Aerospace Sciences*[J], 2018, 97: 22

3 Mahto R P, Gupta C, Kinjawadekar M *et al. Journal of Manufacturing Processes*[J], 2019, 38: 370

4 Nourani M, Milani A S, Yannacopoulos S. *International Journal of Advanced Manufacturing Technology*[J], 2015, 79(9): 1425

5 Woo W, Balogh L, Ungár T *et al. Materials Science and Engineering A*[J], 2008, 498(1-2): 308

6 Xiao W, Wang Y. *Materials Letters* [J], 2021: 129 932

7 Wang W, Han P, Peng P *et al. Journal of Materials Research and Technology*[J], 2020, 9: 5252

8 Gao X, Zhang Z, Wang W *et al. Rare Metal Materials and Engineering*[J], 2016, 45(7): 1857

9 Cao G H, Liu Y X, Zhang D T *et al. Rare Metal Materials and Engineering*[J], 2018, 47(10): 3179

10 Chen Y, Wang H, Ding H *et al. Journal of Materials Engineering and Performance*[J], 2019, 28(5): 2845

11 Chen Y, Li H, Wang X *et al. Journal of Materials Engineering and Performance*[J], 2020, 29(2): 1185

12 Satyanarayana M V N V, Kumar A. *Proceedings of the Institution of Mechanical Engineers Part C-Journal of Mechanical Engineering Science*[J], 2020, 234(22): 4520

13 Chen Y, Jiang Y, Ding H *et al. Journal of Materials Science and Technology*[J], 2018, 34(2): 153

14 Moustafa E B, Melaibari A, Basha M. *Ceramics International* [J], 2020, 46(10): 16 938

15 Guo J, Lee B Y, Du Z *et al. JOM*[J], 2016, 68(8): 2268

16 Mohamadigangaraj J, Nourouzi S, Jamshidi A H. *Measurement* [J], 2020, 165: 108 166

17 Woo W, Choo H, Brown D W *et al. Metallurgical and Materials Transactions A*[J], 2007, 38(1): 69

18 Chen Y, Jiang Y, Zhang F *et al. Transactions of the Indian Institute of Metals*[J], 2018, 71(12): 3077

19 Zhao Y, Huang X, Li Q *et al. International Journal of Advanced Manufacturing Technology*[J], 2015, 78(9-12): 1437

20 Barati M, Abbasi M, Abedini M. *Journal of Manufacturing Processes*[J], 2019, 45: 491

21 Mazaheri Y, Heidarpour A, Jalilvand M M *et al. Journal of Materials Engineering and Performance*[J], 2019, 28(8): 4826

22 Arbegast W J. *Scripta Materialia*[J], 2008, 58: 372

23 Liu F J, Fu L, Chen H Y. *Science and Technology of Welding & Joining*[J], 2018, 23(4): 333

24 Liu F J, Fu L, Chen H Y. *Journal of Materials Engineering and Performance*[J], 2018, 27: 3590

25 Commin L, Dumont M, Masse J E *et al. Acta Materialia*[J], 2009, 57(2): 326

26 Chang C I, Lee C J, Huang J C. *Scripta Materialia*[J], 2004, 57: 509

27 İpekoğlu G, Erim S, Çam G. *Metallurgical and Materials Transactions A*[J], 2014, 45(2): 864

28 Huang Y X, Wan L, Lv Z L *et al. Science and Technology of Welding & Joining*[J], 2016, 21(8): 638

29 Huang Y X, Xie Y M, Meng X C *et al. Materials Science and Engineering A*[J], 2019, 740: 211

30 Humphreys F J. *Acta Materialia*[J], 1997, 45(10): 4231

31 Humphreys F J. *Acta Materialia*[J], 1997, 45(12): 5031

32 Jandaghi M R, Pouraliakbar H, Saboori A *et al. Materials*[J], 2021, 14(5): 1290

33 Li J R, Jiang Q T, Sun H Y *et al. Corrosion Science*[J], 2016, 111: 288

34 King A D, Birbilis N, Scully J R. *Electrochimica Acta*[J], 2014, 121: 394

35 Torbati-Sarraf H, Torbati-Sarraf S A, Chawla N *et al. Corrosion Science*[J], 2020, 174: 108 838

相同速度比搅拌摩擦加工对Al-Mg-Si合金搅拌区微观组织演变、力学性能和腐蚀行为的影响

孙志勇[1]，刘奋军[1,2]，陈海燕[3]

(1. 榆林学院 能源工程学院，陕西 榆林 719000)

(2. 榆林学院 榆林市金属基复合材料与再制造技术重点实验室，陕西 榆林 719000)

(3. 西北工业大学 材料学院，陕西 西安 710072)

摘 要：采用搅拌摩擦加工技术对2 mm厚Al-Mg-Si（6061-T6）合金板材进行加工。研究了具有相同速度比的搅拌摩擦加工对搅拌区微观组织演变、显微硬度分布、拉伸性能和腐蚀行为的影响。结果表明，加工区微观组织如晶粒形貌、平均晶粒尺寸、晶界分布和析出相演变特征具有明显差异，进而对力学性能和腐蚀行为产生显著影响。加工区等轴再结晶晶粒平均尺寸随着加工速度增加而逐渐减小。转速8000 r/min和加工速度800 mm/min工艺下制备的加工区平均晶粒明显细化，析出相分布也更加接近于母材分布特征。最终，该加工区除了耐腐蚀性能轻微改变之外，展现出了较优的力学性能。加工区最大抗拉强度和延伸率分别达281.5 MPa和34.8%，分别为母材的86.3%和122.1%。高速搅拌摩擦加工对腐蚀性能改善不明显，但可有效改善Al-Mg-Si合金的力学性能。

关键词：Al-Mg-Si合金；搅拌摩擦加工；微观组织演变；力学性能；腐蚀行为

作者简介：孙志勇，男，1978生，硕士，副教授，榆林学院能源工程学院，陕西 榆林 719000，E-mail：313537581@qq.com